

RESEARCH

Open Access



The in-vivo dynamics of *Plasmodium falciparum* HRP2: implications for the use of rapid diagnostic tests in malaria elimination

Louise Marquart^{1,2*} , Lachlan Webb¹, Peter O'Rourke¹, Michelle L. Gatton³, Michelle S. Hsiang^{4,5,6}, Michael Kalnoky⁷, Ihn Kyung Jang⁷, Henry Ntuku⁵, Davis R. Mumbengegwi⁸, Gonzalo J. Domingo⁷, James S. McCarthy^{1,2†} and Sumudu Britton^{1,2†}

Abstract

Background: Rapid diagnostic tests (RDTs) that rely on the detection of *Plasmodium falciparum* histidine-rich protein 2 (PfHRP2) have become key tools for diagnosing *P. falciparum* infection. The utility of RDTs can be limited by PfHRP2 persistence, however it can be a potential benefit in low transmission settings where detection of persistent PfHRP2 using newer ultra-sensitive PfHRP2 based RDTs can serve as a surveillance tool to identify recent exposure. Better understanding of the dynamics of PfHRP2 over the course of a malaria infection can inform optimal use of RDTs.

Methods: A previously published mathematical model was refined to mimic the production and decay of PfHRP2 during a malaria infection. Data from 15 individuals from volunteer infection studies were used to update the original model and estimate key model parameters. The refined model was applied to a cohort of patients from Namibia who received treatment for clinical malaria infection for whom longitudinal PfHRP2 concentrations were measured.

Results: The refinement of the PfHRP2 dynamic model indicated that in malaria naïve hosts, *P. falciparum* parasites of the 3D7 strain produce 33.6×10^{-15} g (95% CI 25.0–42.1 $\times 10^{-15}$ g) of PfHRP2 in vivo per parasite replication cycle, with an elimination half-life of 1.67 days (95% CI 1.11–3.40 days). The refined model included these updated parameters and incorporated individualized body fluid volume calculations, which improved predictive accuracy when compared to the original model. The performance of the model in predicting clearance of PfHRP2 post treatment in clinical samples from six adults with *P. falciparum* infection in Namibia improved when using a longer elimination half-life of 4.5 days, with 14% to 67% of observations for each individual within the predicted range.

Conclusions: The updated mathematical model can predict the growth and clearance of PfHRP2 during the production and decay of a mono-infection with *P. falciparum*, increasing the understanding of PfHRP2 antigen dynamics. This model can guide the optimal use of PfHRP2-based RDTs for reliable diagnosis of *P. falciparum* infection and re-infection in endemic settings, but also for malaria surveillance and elimination programmes in low transmission areas.

Keywords: Rapid diagnostic tests, *Plasmodium falciparum*, Histidine rich protein, Antigen dynamics, Elimination and surveillance

Background

Rapid diagnostic tests (RDTs) have become key tools for diagnosing clinical malaria, especially in resource limited settings. These lateral flow antigen capture based assays rely on detection of at least one of three parasite

†James S. McCarthy and Sumudu Britton are joint senior authors

*Correspondence: l.marquart@uq.edu.au

² University of Queensland, Brisbane, QLD, Australia

Full list of author information is available at the end of the article



antigen biomarkers: *Plasmodium falciparum* histidine rich protein 2 (*PfHRP2*), lactate dehydrogenase (LDH), and aldolase. The majority of RDTs used for diagnosis of *P. falciparum* rely on detection of *PfHRP2*, either alone or in combination with pan-*Plasmodium* LDH (pLDH) [1].

Two major shifts in the approach to malaria control have highlighted gaps in the existing diagnostic toolkit pertaining to RDTs. First, in 2007 the World Health Organization (WHO) in conjunction with the Roll Back Malaria partnerships, and the Bill & Melinda Gates Foundation committed to the ambitious goal of malaria eradication [2]. However, new strategies and tools will be required to achieve this goal. For example, mass or focal screen and treat strategies, rely on the use of sensitive, specific and field ready tests coupled with administration of effective anti-malarial medication [3]. However, data from studies where RDTs have been used for this purpose suggest that they are insufficiently sensitive to achieve the required reduction in cases [4, 5].

Second, in 2010 the WHO Guidelines for the treatment of malaria changed such that parasitological confirmation of infection, using either RDTs or microscopy, was required prior to treatment [6]. However, as with all diagnostic tools, RDTs have their limitations. Importantly *PfHRP2* has been shown to persist for up to 36 days after curative treatment [7, 8]. This undermines the feasibility of using *PfHRP2*-based RDTs to detect re-infection in treated patients in regions of high malaria endemicity [9, 10] and limits their utility in post treatment follow up, for example in pregnant women [11]. Antigen persistence may also delay appropriate treatment for other causes of febrile illness that may be incorrectly attributed to malaria [12–14].

However, persistent antigenaemia is a potential benefit in low transmission settings, where detection of persistent *PfHRP2* using newer ultra-sensitive *PfHRP2* based-RDTs (usRDT) [15] may provide a measure of recent parasite infection as part of malaria surveillance and elimination programs. While the newer assays do not overcome the problem of false negative results due to *hrp2* gene deletions [16, 17], a better understanding of the dynamics of *PfHRP2* during the course of infection, both before and after treatment, is essential to better inform optimal utilization of *PfHRP2*-based RDTs.

Synthesis of *PfHRP2* by *P. falciparum* parasites has been shown, in vitro, to begin within 2 h of initiation of the intraerythrocytic asexual lifecycle, i.e. in early ring stage [18], with the greatest production of *PfHRP2* per parasite occurring between ring and trophozoite stages, and absolute production varying in a strain-dependent manner [19]. Although *PfHRP2* has been shown to be at highest concentration in the whole blood compared with plasma [20], it has also been suggested that measurement

of the plasma level of *PfHRP2* may be a useful way to estimate *P. falciparum* biomass compared with measurement of parasitaemia due to sequestration of late stage parasites [21]. Central to the potential use of *PfHRP2* to calculate biomass is the clearance half-life of *PfHRP2*, for which estimates have ranged from 1.10 days [22] up to 4.7 days [23, 24] each of which have been based on limited sampling frequency.

A previous mathematical model of the kinetics of *PfHRP2* [25] was developed by simulating the production and clearance of *PfHRP2* during a single, relatively synchronous infection of *P. falciparum*. However, the model used quantitative measurement of antigen from only three subjects and utilized key parameter values as reported in the literature. In this study, the mathematical model is refined by using a larger set of samples with more intensive sampling, and the use of a more sensitive assay [26] to better quantify *PfHRP2* levels. The utility of the new mathematical model was validated against longitudinal *PfHRP2* values measured in a cohort of patients from Namibia who received anti-malarial treatment after mosquito-acquired infection. This mathematical model provides a framework for individualized prediction of *PfHRP2* during a mono-infection with *P. falciparum*, improving the understanding of diagnostic marker dynamics to guide the optimal use of *PfHRP2*-based RDTs.

Methods

Study datasets

Two datasets were used in this study. First, data from an induced blood-stage malaria (IBSM) study were used to update the original *PfHRP2* mathematical model [25]. Secondly, data from a longitudinal cohort study conducted in Namibia were used to assess performance of the model.

Parasitaemia and *PfHRP2* concentration data used to update the original HRP2 mathematical model [25] were from 15 malaria-naïve healthy subjects who participated in an IBSM study (NCT02389348 [27], NCT02431637 [28], NCT02431650 [28], NCT02573857 [29]), conducted by the clinical unit Q-Pharm Pty Ltd at QIMR Berghofer Medical Research Institute between 2015 and 2016. Briefly, subjects were inoculated intravenously on Day 0 with human red blood cells infected with approximately 1800 or 2800 viable 3D7 *P. falciparum*. Parasitaemia was monitored by twice daily blood sampling from Day 4 until treatment on Day 7. Subjects were admitted to the clinical unit, treated with either 200 mg artefenomel/50 mg DSM265, 480 mg piperazine or 400 mg DSM265 (details in Additional file 1: Material S1), and observed for at least 72 h prior to continuing outpatient monitoring for safety and

clearance of all parasites prior to discharge from the study. Model development and analysis were restricted to data corresponding to blood samples collected from Day 4 until Day 11 following inoculation, as this time-period captured the production and decay of the first infection without recrudescence or the appearance of gametocytes.

Data from a longitudinal cohort study were used to validate the updated *PfHRP2* model. This study was conducted in the Zambezi Region, Namibia, a low transmission *P. falciparum* dominant setting. Malaria-infected individuals testing positive by RDT [CareStart™ Malaria *Pf*PAN (HRP-2/pLDH) Antigen, AccessBio] were recruited from health facilities and community test and treat activities. After receiving treatment with artemisinin-based combination therapy (ACT) (artemether–lumefantrine) and low dose primaquine, blood sampling was conducted weekly until testing by the standard RDT and usRDT were both negative for 2 consecutive weeks. A sample of study participants was selected to assess the applicability of the *PfHRP2* model to predict *PfHRP2* over time after treatment administration. The sample included individuals with a *P. falciparum* mono-infection, confirmed using a PCR assay targeting the *cox3* gene [30] on Day 0 samples; subjects aged between 23 and 27 years were selected to correspond with the interquartile range of the ages of the IBSM study participants. The parasitaemia growth and clearance were simulated for each individual to be used as input into the mathematical model; the body weights of study individuals were simulated from an estimated gender-and-age specific weight curve for Namibian individuals from the 2003/2004 Namibia Household Income and Expenditure Survey [31]. Further detail about the data used for the HRP2 modelling of the Namibia individuals is in Additional file 1: Material S2. As *PfHRP2* elimination half-life can differ depending on parasite strain [19] and geographic location [24], and the potential effect of anti-HRP2 antibodies [32], additional modelling was applied to the Namibia sample data using an elimination half-life of 4.5 days as estimated from a study in neighbouring Angola [24].

The IBSM study was approved by the QIMR Berghofer Medical Research Institute Human Research Ethics Committee. The study protocol for the Namibia longitudinal cohort study was approved by the Research Unit of the Ministry of Health and Social Services of Namibia, the University of Namibia Research Ethics Committee and the University of California, San Francisco Committee for Human Research. All participants recruited for the study or their parents/guardians provided written consent.

Measurement of *PfHRP2* concentration and parasitaemia

The concentration of *PfHRP2* in each sample was measured using Q-Plex-based enzyme linked immuno-sorbent assays (ELISAs) [15, 26]. These assays are a multiplex array immunoassay (Quansys Biosciences) using a solid phase in defined areas coated with capture antibodies specific for common biomarkers, *PfHRP2* and C-reactive protein (CRP). Briefly, for *PfHRP2* measurement, a 50 µL sample (whole blood sample and sample diluent of 1:4) was incubated for an hour and after washing away any unbound proteins, a detection mixture containing biotinylated antibody was added and incubated for an hour or three hours. After washing away unbound biotinylated antibody, the plate was incubated with streptavidin–horseradish peroxidase for 20 min. Following the addition of a chemiluminescent substrate, the signal on this array was captured by Q-view imager. *PfHRP2* concentration was back calculated from chemiluminescent signals fit to a 5-parameter logistic curve estimating luminescence and *PfHRP2* concentration. IBSM samples were measured by 2-plex and Namibia samples by 4-plex assays on this platform.

Parasitaemia for the IBSM participants was measured using a 18s rRNA quantitative PCR (qPCR) assay as previously described [33]. The parasitaemia for individuals from the Namibia study was measured using a qPCR targeting the varATS region of *P. falciparum* [34]. DNA was extracted from thawed packed red blood cells using the Quick-DNATM miniprep kit (Zymo Research Coup) resuspended in 100 µL of water.

Modelling *PfHRP2* kinetics

The original mathematical model [25] assumed the production of *PfHRP2* occurred early in the asexual cycle, with all the protein remaining within the infected RBC (iRBC) until the time of schizont rupture, when it is instantaneously released into the circulation. Briefly, the model uses the number of parasites replicating (i.e. schizonts rupturing) at a given time during an infection to estimate the corresponding *PfHRP2* concentration. The model assumes that elimination of *PfHRP2* is a continuous first-order decay process,

$$d_k = \exp\left[\frac{\ln(0.5)k}{t_{\frac{1}{2}}}\right],$$

where d_k is the proportion of *PfHRP2* remaining k days after it was produced, and $t_{\frac{1}{2}}$ is the half-life of *PfHRP2*. The absolute amount of *PfHRP2* circulating the body at any day during an infection, H_t , was calculated using:

$$H_t = f \sum_{j=1}^t d_{t-j} p_j,$$

where t is time in days and $t = 1$ is the first schizogony, p_j is the number of replicating parasites circulating in the host on the j th day, and f is the amount of PfHRP2 produced per parasite per lifecycle. Two scenarios for PfHRP2 distribution within the body were considered. The first assumed that PfHRP2 is water soluble and equally distributed throughout the extracellular fluid (ECF). The second assumed that PfHRP2 is distributed in the total blood volume (BV). These two provided the minimum and maximum concentration of circulating PfHRP2, T_{min_i} and T_{max_i} .

Four aspects of the original model were considered to be updated: the amount of PfHRP2 produced per parasite per life cycle (f); the life cycle duration of the *P. falciparum* parasites; individual-specific fluid volumes for the distribution of PfHRP2; and the elimination half-life of PfHRP2 ($t_{\frac{1}{2}}$). These model aspects were updated separately and also in combination. Sensitivity analyses were performed on the final model to assess robustness of the final model to changes in values of f and $t_{\frac{1}{2}}$. Analyses and model fitting were performed in R (Version 3.6.1).

Amount of PfHRP2 produced per parasite per life cycle

Following the methodology detailed in Marquart et al. [25], pre-treatment data from the IBSM study were used to calculate an estimate of the amount of PfHRP2 produced per parasite life cycle (f^*). The original estimate of the amount of PfHRP2 produced, f_0 , was set to 5.2×10^{-15} g [19]. This value was adjusted using a scaling factor (m). The optimal value of the scaling factor, which produced the minimum residual sum of squares (RSS) between the observed PfHRP2 concentration and the predicted PfHRP2 for $f_0 \times m$, was calculated for each IBSM individual. The mean scaling factor, \bar{m} , was used to determine the new estimate of the amount of PfHRP2 produced per parasite, $f^* = f_0 \bar{m}$, to be utilised in subsequent models.

Life cycle duration of the 3D7 strain of *P. falciparum* parasite

The life cycle duration of the 3D7 strain used in the IBSM studies is estimated to be 39 h [35]. To account for the shorter life cycle than the previously assumed 48 h, the model was modified to consider which available time-points would contribute to the peaks of an approximately 40 h life cycle.

Body fluid volume

Individualized blood volumes (L) were estimated by using body weight (kg) as, $BV = 0.07 \times \text{weight}$ [36]. Two individualised ECF volumes (L) based on body weight (kg) were considered, the first estimated as $ECF = 0.2 \times \text{weight}$ [37] and the second was gender specific with individualised ECF volumes

estimated as $ECF = 0.22 \times \text{weight}$ for females, and $ECF = 0.245 \times \text{weight}$ for males [36].

Elimination half-life of PfHRP2 in 3D7 *P. falciparum*

The elimination half-life of PfHRP2 in *P. falciparum* infection was estimated using data measured 12 h apart from treatment administration on Day 7 to Day 11. Estimation of the elimination half-life was restricted to the subset of 10 individuals who had a maximum PfHRP2 concentration exceeding 300 pg/mL. For each individual, the elimination rate λ , was estimated by fitting a linear regression to the last n^* time-points of the natural log PfHRP2 concentration over time with the final data point included in the regression being the first occurrence of the concentration value below the limit of detection (LOD). Five values of n^* were considered ranging from 3 to 7. The slope coefficient of the regression model that corresponded to the largest adjusted R-squared for each individual was determined as the elimination rate. The mean elimination rate ($\bar{\lambda} = \frac{1}{10} \sum_{i=1}^{10} \lambda_i$) was used to estimate the elimination half-life of PfHRP2, by: $t_{\frac{1}{2}} = \frac{\ln(2)}{\bar{\lambda}}$. Regression models were estimated for each subject using the *pkexamine* command within Stata 13.0 (Stata Corporation, College Station, TX).

Measures to assess model fit

Three metrics were used to evaluate the fit of the model. The first metric is the number of observed PfHRP2 measurements for each subject that were between the minimum and maximum levels of the predicted PfHRP2 (T_{min_i} and T_{max_i}). The summation over all subjects is calculated as a total number of observed PfHRP2 measurements within the predicted range for the model under consideration. The second metric calculates the residual sum of squares of the model for each subject (RSS_i), taking the residual of observed \log_{10} PfHRP2 concentration from the mean value of the minimum and maximum predicted \log_{10} PfHRP2 concentrations. The total RSS (TRSS) is the summation of RSS_i over all subjects. The third metric, calculated at the individual level, is the root mean square error (RMSE), calculated as the standard deviation of the residuals from the mean value of the minimum and maximum predicted \log_{10} PfHRP2.

Results

Model development

Demographic data for the 15 individuals from the IBSM study used for model fitting are outlined in Table 1. All individuals were treated with an anti-malarial on Day 7. The majority of individuals were male (11/15, 73%) and the median age was 24 (Interquartile range [IQR]: 23–27) years. The mean weight (range) for females was 68.9

Table 1 Summary characteristics of the 15 IBSM individuals used for model development

Characteristic	n (%)
Gender	
Male	11 (73%)
Female	4 (27%)
Age	
18–24	9 (60%)
25–29	4 (27%)
30–55	2 (13%)
Weight (kg)	
50–69	4 (27%)
70–89	9 (60%)
90–110	2 (13%)
Pre-treatment peak parasitaemia (parasites/mL)	
0–9999	5 (33%)
10,000–19,999	5 (33%)
20,000–29,999	3 (20%)
30,000–61,357	2 (13%)
Pre-treatment peak PfHRP2 (pg/mL)	
0–299	5 (33%)
300–599	3 (20%)
600–899	4 (27%)
900–2163	3 (20%)
Anti-malarial drug administered at day 7 post inoculation	
200 mg artefenomel + 50 mg DSM265	3 (20%)
480 mg piperaquine	5 (33%)
400 mg DSM265	7 (47%)

(58.2–75.9) kg and for males was 79.2 (65.0–101.6) kg. During the pre-treatment phase, the median peak parasitaemia (range) was 15,849 (1230–61,357) parasites/mL, and the median peak PfHRP2 concentration (range) was 535 (37–2163) pg/mL. The relationship between parasitaemia and PfHRP2 over the course of the study period for each of the anti-malarial drug groups is summarized in Fig. 1.

Updating the HRP2 model

The mean scaling factor from the 15 individuals was 6.5 (95% CI 4.8–8.1), corresponding to an estimated amount of PfHRP2 produced per parasite life cycle, f^* , of 33.6×10^{-15} (95% CI 25.0–42.1 $\times 10^{-15}$) g. This value was used in the Base Model, and all subsequent parameters expanded upon this model. The performance of the models considered during the model development process is presented in Table 2. The final model was selected based on model performance as evaluated by the minimum TRSS and the maximum number of points within range.

The Base Model was similar to the original model of [25] and assumed a 48-h life cycle duration for the 3D7 *P. falciparum* strain, a blood volume of 5 L, an ECF volume of 14 L and a PfHRP2 elimination half-life of 3.67 days. Improvements to the goodness of fit for updates to each of these parameters are given in Table 2. Changing the duration of the life cycle of the 3D7 parasite to 40 h (Model 1, Table 2) did not result in any improvement to the Base Model. Five of the 15 individuals had blood volume estimates based on body weight which were below the previously assumed 5 L (range 4.1–7.1 L) and 14 had sex-weight specific ECF estimates above the previously assumed 14 L (range 12.8–24.9 L). Therefore, incorporating the individualised body fluid calculations based on weight and sex improved the model accuracy (Models 2 and 3, Table 2).

The PfHRP2 concentrations over time from the 10 individuals who had maximum PfHRP2 concentrations exceeding 300 pg/mL (Fig. 2) were used to estimate an elimination half-life of 1.67 days (95% CI 1.11–3.40 days) and used to update the models (Models 4–6, Table 2). The performance of the HRP2 model improved with the updated elimination half-life estimates of 1.67 days and the lower confidence interval limit of 1.11 days, with respectively 21% or 25% of observed PfHRP2 concentrations within the predicted range of PfHRP2 concentrations (Table 2).

A combined model was considered to assess the simultaneous impact of incorporating sex-weight specific estimates of body fluid volumes and updating the elimination half-life of 1.67 days (Model 7, Table 2). The combined model substantially improved the accuracy of the model in comparison to the Base Model, increasing the proportion of observed PfHRP2 concentrations within the predicted range of PfHRP2 concentrations from 13 to 27%. This model utilising the sex-specific weight in the calculation of the ECF volume performed best and was considered the Final Model. The model fits from the Base Model and Final Model for two individuals are shown in Fig. 3 and model fits for all 15 individuals are shown in Additional file 1: Table S1 and Fig. S1.

Sensitivity of the Final Model to changes in key parameters was assessed by considering different models whereby the assumed amount of PfHRP2 produced per parasite (f^*) and the PfHRP2 elimination half-life estimates ($t_{1/2}$) varied based on the estimated lower and upper bounds of the 95% confidence intervals (Models 8–11, Table 2). The model was sensitive to the changes in f^* , with the use of the lower bound of the confidence interval for f^* of 24.97×10^{-15} g improving the model accuracy to 31% of PfHRP2 observations within the predicted range (Model 9, Table 2). The Final Model was also sensitive to the elimination half-life, with a smaller magnitude

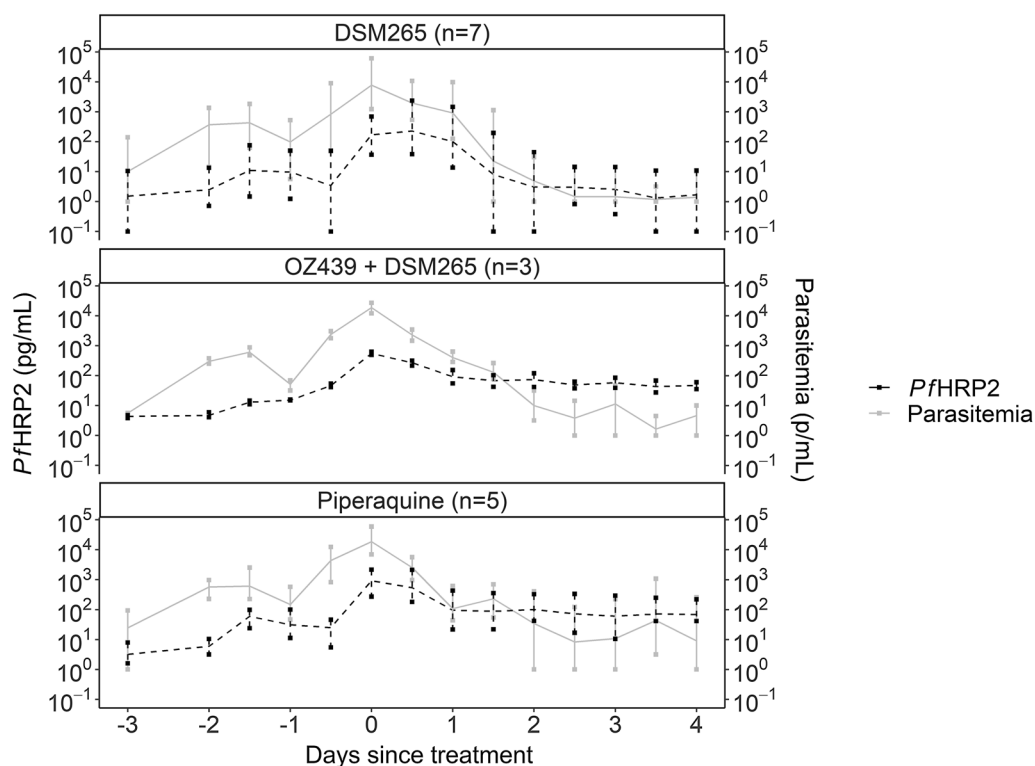
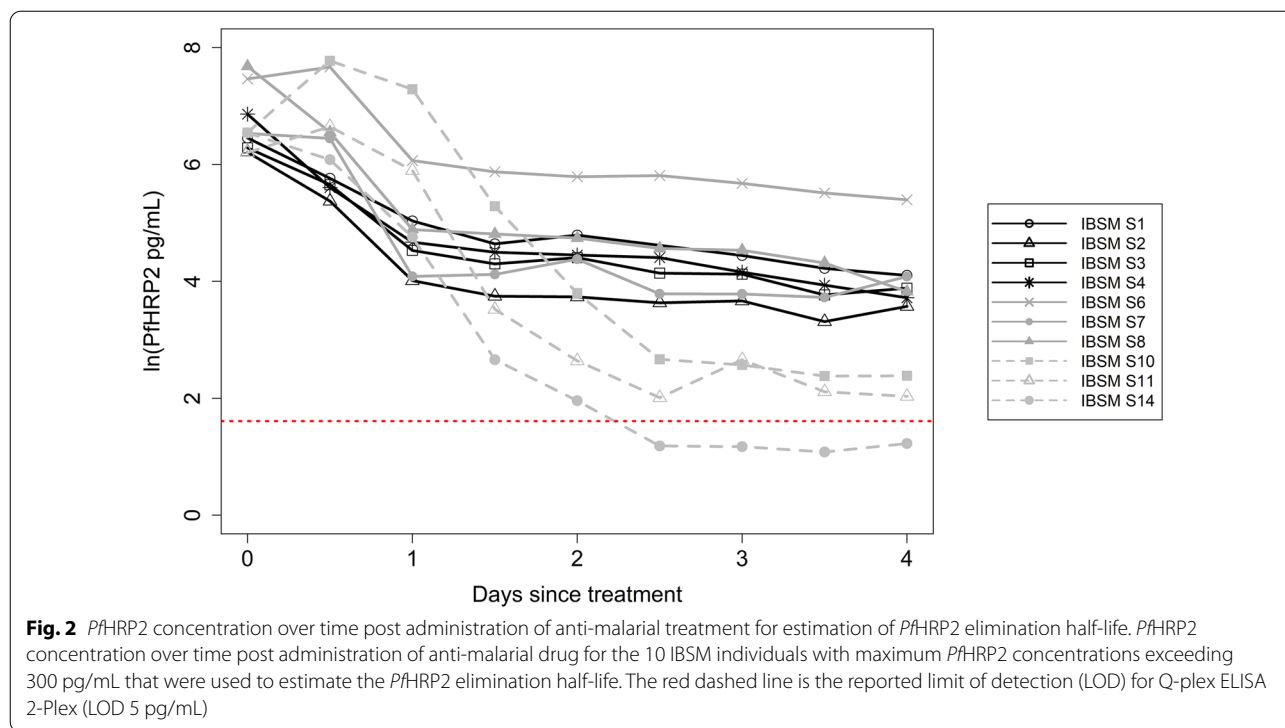


Fig. 1 Parasitaemia and *PfHRP2* concentration over study period for three anti-malarial treatments in IBSM studies. Relationship between mean parasitaemia (Grey solid line) and mean *PfHRP2* concentration (Black dashed line) over the study period used for model development for each of the three anti-malarial treatments in the IBSM study. Bars at each time-point represent minimum and maximum

Table 2 Summary of each model aspect evaluated during the development and sensitivity phases, with performance measures

Phase	Model number	Description	TRSS	Number (%) of observations in predicted interval
Development	Base	Previously published model, with updated f^* value of 33.6	176.2	27 (13%)
	1	40 h parasite life cycle	185.5	27 (13%)
	2	Body fluid estimated by weight. $BV = 0.07 \times \text{weight}$, $ECF = 0.2 \times \text{weight}$	171.5	30 (14%)
	3	Body fluid estimated by weight and sex. $BV = 0.07 \times \text{weight}$, $ECF = 0.245 \times \text{weight}$ for males and $ECF = 0.22 \times \text{weight}$ for females	164.2	37 (18%)
	4	Elimination half-life estimate of 1.67 days	131.1	43 (21%)
	5	Elimination half-life lower bound of 95% CI of 1.11 days	102.7	51 (25%)
	6	Elimination half-life upper bound of 95% CI of 3.40 days	172.7	28 (13%)
	7 (Final)	Body fluid estimated by weight and sex. $BV = 0.07 \times \text{weight}$, $ECF = 0.245 \times \text{weight}$ for males and $ECF = 0.22 \times \text{weight}$ for females and elimination half-life of 1.67	122.6	57 (27%)
Sensitivity	8	Final model with the upper confidence bound of the 95% CI for f^* , $f = 42.18$	141.1	49 (24%)
	9	Final model with the lower confidence bound of the 95% CI for f^* , $f = 24.97$	104.8	64 (31%)
	10	Final model with the upper confidence bound of the 95% CI for half-life, 3.40 days	160.9	37 (18%)
	11	Final model with the lower bound of the 95% CI for half-life, 1.11 days	97.2	57 (27%)

Performance measures evaluated during the development and sensitivity phases were the total residual sum of squares (TRSS) and the number (%) of *PfHRP2* observations within the range of the predicted minimum and maximum *PfHRP2* concentrations as generated from the models. Model 7 is considered the final model (bold)



of TRSS but having the same model accuracy when the upper bound of $t_{\frac{1}{2}}$ of 1.11 days was used (Model 11, Table 2).

Application of *Pf*HRP2 model to clinical samples from Namibia

The Final Model was applied to the simulated parasitaemia growth and clearance data from a total of six individuals from the Namibia study that met the selection criteria for the validation study. The six individuals all had symptomatic *P. falciparum* mono-infection and were recruited from health facilities before receiving treatment. The details of the 6 individuals are shown in Table 3. The sample comprised of an equal number of males and females aged 24 or 25 years. The estimated weights of the individuals extracted from the sex-and-age specific curves [31] ranged from 56.5 to 62 kg. Parasitaemia at time of enrolment ranged from 99,500 to 49,346,000 parasites/mL, and *Pf*HRP2 concentrations ranged from 2313 to 1.1×10^{10} pg/mL. The follow up duration ranged from 21 to 84 days.

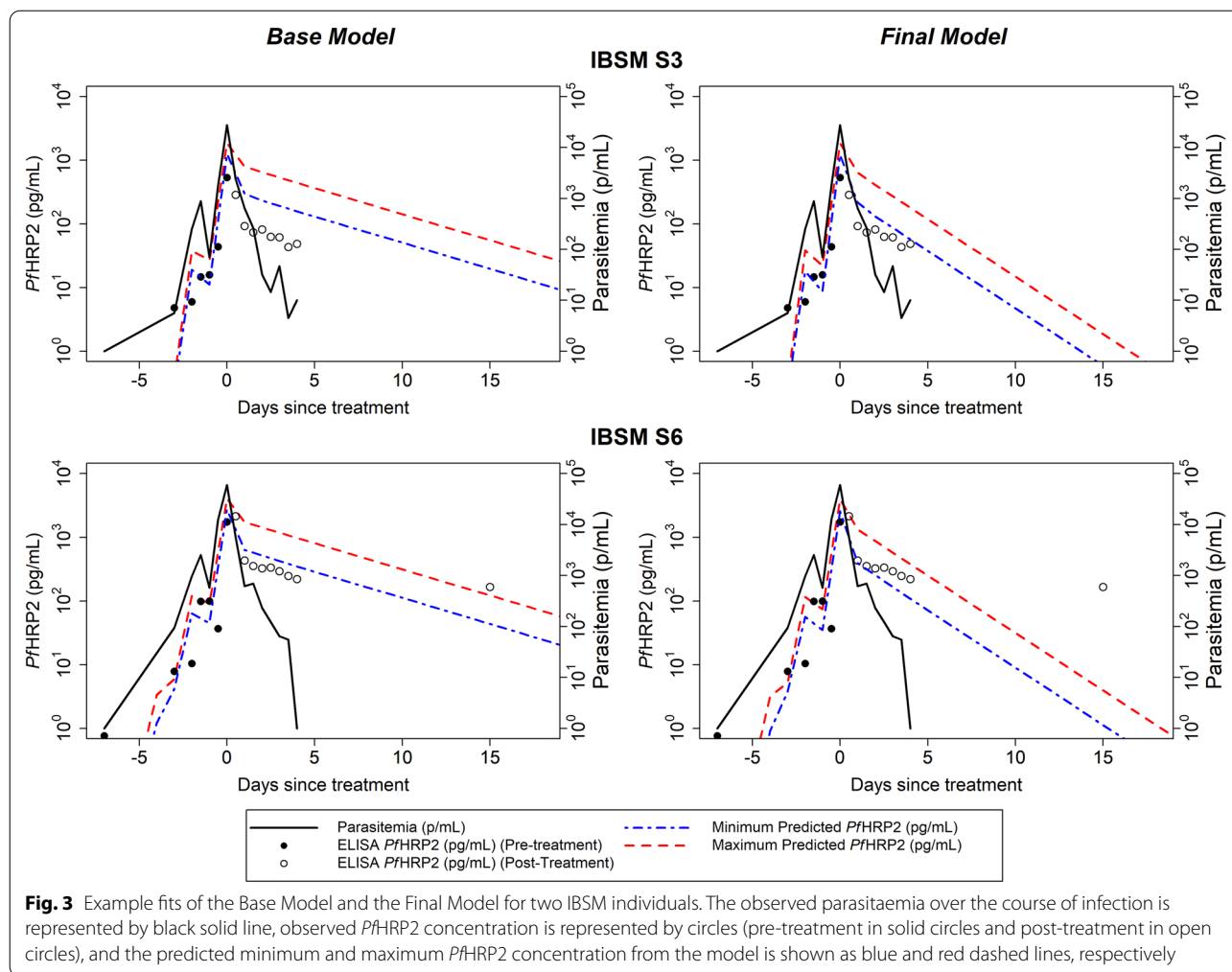
The predicted amount of circulating *Pf*HRP2 ($H_{min,t}$ and $H_{max,t}$) estimated using the Final Model based on the 3D7 IBSM estimated elimination half-life of 1.67 days underestimated the observed *Pf*HRP2 clearance (Additional file 1: Table S3, Figs. S2, S3) in the Namibian individuals. When the model was modified to use an elimination half-life of 4.5 days, as reported in neighbouring Angola

[24], the trend of *Pf*HRP2 clearance over time was better captured with 14% to 67% of observed *Pf*HRP2 concentrations for each individual within the minimum and maximum predicted *Pf*HRP2 concentrations (Table 3, Fig. 4).

Using a limit of detection (LOD) of 800 pg/mL for the standard HRP2-based RDT [1], the model predicted that standard RDT positivity would continue for 14 to 54 days and usRDT would remain above its LOD of 80 pg/mL [15] for 29 to 69 days following study enrolment. The number of days *Pf*HRP2 was predicted to be above 800 pg/mL was underestimated for 3 of the 6 individuals, and the difference in the predicted and observed time above 800 pg/mL ranged between -6 and 11 days. For the 3 individuals that were observed to have *Pf*HRP2 below 80 pg/mL during the study, the model predicted the number of days above the threshold ranged between -7 and 3 days of that observed.

Discussion

In this study, a previously published mathematical model [25] was updated using data from 15 subjects with experimental malaria infection to more accurately describe the dynamics of *Pf*HRP2 during a *P. falciparum* mono-infection. The updated model, when applied to clinical samples from six adults with a *P. falciparum* infection in Namibia using a *Pf*HRP2 half-life of 4.5 days as had been previously reported in the region [24], performed



well in predicting the concentration changes in *PfHRP2* over time. The predicted *PfHRP2* concentrations were subsequently used to estimate the duration that standard RDTs and usRDTs would be expected to remain positive in these individuals, thereby providing a framework for interpreting the results of *PfHRP2* based RDTs where *PfHRP2* persists following treatment.

A key parameter in modelling the dynamics of *PfHRP2* antigenaemia was the amount of *PfHRP2* produced per parasite life cycle (f). Using the combination of a sensitive ELISA to measure whole blood concentration to quantify *PfHRP2* and frequent sampling prior to treatment, in this study it was estimated that 33.6×10^{-15} (range: $11.3-71.1 \times 10^{-15}$) g of *PfHRP2* is produced in vivo per parasite per life cycle. This is approximately sixfold higher than the previously reported median value of 5.2×10^{-15} (range: $1.1-13.0 \times 10^{-15}$) g [19], but lower than the estimate of 141×10^{-15} g from the original model [25].

Another key parameter for describing *PfHRP2* dynamics was the estimated *PfHRP2* elimination half-life,

which in this study was found to be 1.67 (95% CI 1.11–3.40) days in malaria naïve healthy volunteers undergoing experimental infection. This is shorter than the 3.67 days previously reported in adult patients with a mixture of uncomplicated or severe malaria [23] who had been treated with ACT or quinine depending on the severity of infection with plasma *PfHRP2* measured on days 1, 3, 7, 14 and 21 [23]. The plasma half-life of *PfHRP2* reported by Hendriksen et al. was 1.10 (95% CI 0.91–1.29) days from a sample of 30 patients [22]. However, this estimate was based on 3 time points (0, 3 and 7 days post treatment). Plucinski et al. also reported a median half-life of *PfHRP2*, measured by bead-based assay technology, in the peripheral circulation among symptomatic patients after treatment for uncomplicated *P. falciparum* malaria, of 4.5 (IQR 3.3–6.6) days, 4.7 (IQR 4.0–5.9) days and 3 (IQR 2.1–4.5) days in Angola, Tanzania and Senegal, respectively [24]. These were persons from malaria endemic regions under the age of 10 year (Angola and Tanzania) and between 4 and 20 years

Table 3 Namibia study participant characteristics and performance of *PfHRP2* model with half-life of 4.5 days

ID		Characteristics					Model performance					
Age	Sex	Estimated weight (kg)	Enrolment parasitaemia (p/mL) × 10 ⁶	Enrolment <i>PfHRP2</i> (pg/mL) × 10 ⁵	Follow up duration (days)	Number (%) observations in predicted interval	RSS	RMSE	Predicted days above 800 pg/mL	Last day observed above 800 pg/mL	Predicted days above 80 pg/mL	Last day observed above 80 pg/mL
F1	24	Male	61	9.46	0.83	84	2 (14%)	10.77	0.877	44.9	59.9	63
F2	25	Male	62	2.88	0.33	63	5 (50%)	1.56	0.395	34.3	49.3	42
F3	25	Female	58	0.10	0.002	21	1 (25%)	0.41	0.320	14.1	29.1	–
F4	24	Male	61	22.61	0.40	56	6 (67%)	1.43	0.399	47.7	62.7	–
F5	25	Female	58	0.39	3.66	28	3 (60%)	5.57	1.055	23.3	38.3	–
F6	24	Female	56.5	49.35	10,931.8	77	4 (31%)	19.3	1.217	54.9	69.9	70

Participant characteristics and model performance of the updated model with *PfHRP2* half-life estimate of 4.5 days applied to 6 individuals aged between 23 and 27 years from the study in Namibia in participants with *P. falciparum* mono-infection

RSS residual sum of squares, RMSE root mean standard error calculated on the mid-point of the minimum and maximum predicted *PfHRP2* concentrations—no observations were observed below 80 pg/mL so the last day above the threshold of 80 pg/mL was not able to be reported

(Senegal) who had higher parasitaemia at treatment with ACT ($100,000\text{--}2 \times 10^8$ parasites/mL), and were sampled at days 0, 3, 7 and weekly for 28–42 days [24]. Similar characteristics were observed in the adults from the Namibia field study presented here (parasitaemia of $100,000\text{--}5 \times 10^7$ parasites/mL and artemisinin-based combination treatment).

There are several potential explanations for the differences in *PfHRP2* elimination half-life between this IBSM study and others. These include the effects of immunity, type of anti-malarial treatment used and gametocytaemia. Immunity to malaria is known to sustain higher parasitaemia but also accelerate parasite clearance following treatment [38] with differences evident in children compared with adults [39] but it is not known how this impacts *PfHRP2* clearance. Subjects in this IBSM study were malaria naïve, therefore, it may be postulated that this could impact on clearance of infection and, as a result, of *PfHRP2*. In addition, the anti-malarial agent might influence antigen clearance, with some studies suggesting that treatment with ACT may result in faster *PfHRP2* clearance [40], more prolonged clearance of *PfHRP2* [7] or no difference in clearance [20, 41] compared to non-artemisinin-based combination treatments as used in the IBSM study. Finally, in this IBSM study subjects were sampled more frequently until day 4 post treatment but prior to the development of gametocytes. However, *PfHRP2* is known to be produced by gametocytes in a stage-specific manner [42] and gametocytaemia has been associated with false positivity in RDTs based on *PfHRP2* and pan-malarial antigens, particularly among patients treated with chloroquine and sulfadoxine–pyrimethamine compared with artesunate [7]. These reasons may contribute to the improvement in the model performance observed for the ACT-treated subjects in the Namibia cohort when the half-life of 4.5 days was used rather than the half-life estimate derived from the IBSM subjects treated with non-artemisinin-based combination treatments. Further research into the factors that contribute to these differences in elimination half-life are essential to further understand the dynamics of *PfHRP2*.

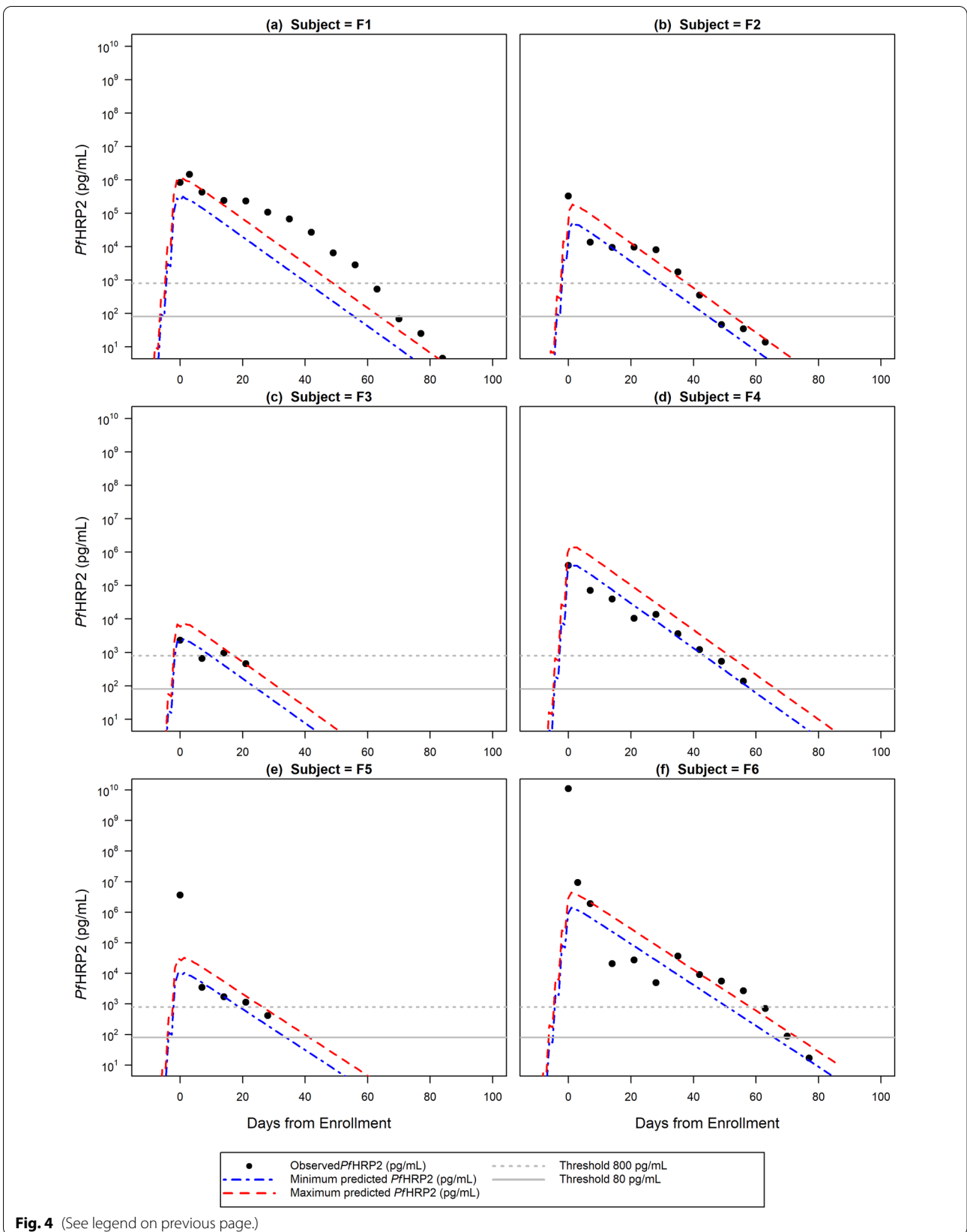
This study has several limitations. First, the *PfHRP2* elimination half-life estimates for the 3D7 strain presented here were determined using ten IBSM

individuals and assumes that *PfHRP2* elimination was initiated instantaneously after treatment administration. Further, it was assumed that there were no treatment effects, no differences in the parasite clearance rate between the four different non-artemisinin based antimalarial treatments and that the anti-malarial treatment cleared all stages of the parasite. Similar to other studies [24], it was assumed in this study that *PfHRP2* is cleared by first order kinetics. However, Reichert et al. found that *PfHRP2* clearance following ACT could be best modelled with biphasic clearance kinetics [43]. In addition, splenic pitting following ACT treatment has been suggested as a mechanism that may explain prolonged *PfHRP2* persistence despite rapid parasite clearance with artemisinin-based combination treatment [20] and could be postulated to be a contributing factor to the difference in clearance kinetics and the longer clearance half-life in ACT treated patients compared to the shorter *PfHRP2* half-life found in this study where the treatments were with non-ACT anti-malarial agents. Further, this study assumed an absence of gametocytaemia for the purpose of developing model parameters. Therefore, if indeed *PfHRP2* accumulation is life cycle stage and strain specific or if *PfHRP2* half-life varies by geographic location, applicability of this model may be improved with delineation of these specific parameters.

This model has been developed using data from malaria-naïve subjects challenged with a single infection of the 3D7 strain of *P. falciparum* and has been applied to six individuals from Namibia to illustrate the potential use of a model to predict *PfHRP2* dynamics. However, further validation is required for predicting *PfHRP2* in different low and high transmission epidemiologic settings and in symptomatic and asymptomatic malaria patients. It is anticipated that in clinical cases of malaria, *PfHRP2* concentration will be higher and subject to influence by the interplay between host age, splenic function and immunity that influence parasite replication as well. Even under the relatively controlled experimental conditions of IBSM studies, the *PfHRP2* elimination rates vary substantially, reflective of the broad range of *PfHRP2* to parasite density observed previously in comparison to lactate dehydrogenase [26]. Therefore, future work is needed to explore the kinetics of *PfHRP2* during clinical infection, recrudescence, chronic

(See figure on next page.)

Fig. 4 Fits of the final model with elimination half-life of 4.5 days to the Namibia study. Fits of the final *PfHRP2* model with elimination half-life of 4.5 days to the 6 individuals from the Namibia study, with observed *PfHRP2* concentration represented by closed circles, and minimum and maximum predicted *PfHRP2* concentration represented by the blue and red dashed lines, respectively. The dashed grey horizontal line represents the threshold of 800 pg/mL and the solid grey horizontal line represents the threshold of 80 pg/mL which correspond to the positivity threshold of an RDT and usRDT, respectively



infections, in infections with different strains of *P. falciparum* and following treatment with anti-malarial agents with different parasite clearance efficacy in order to fully elucidate *PfHRP2* dynamics.

Nevertheless, our model substantially increases the current understanding of *PfHRP2* antigen dynamics. This is crucial for informing optimal use of *PfHRP2*-RDTs for reliable diagnosis of *P. falciparum* infection and re-infection in high endemic settings. Application of this model to a subset of patients treated with rapidly schizontocidal drugs facilitated estimation of how long *PfHRP2* might persist, at an individual level, and be above the detectable threshold for *PfHRP2*-based RDTs. Such application could assist in determining when *PfHRP2*-based RDT positivity reflects previous treatment as opposed to re-infection. Reichert et al. also demonstrated a difference in the ratio of *PfHRP2* to LDH prior to treatment compared with after treatment suggesting that such differences in dynamics of these two antigens could inform the better application of usRDTs for the differentiation of prolonged clearance of treated infection from re-infection [43]. Expanding the IBSM model to include LDH dynamics could at a first instance inform these observations and better inform the use of usRDTs for differentiating infection from re-infection in high transmission settings. Additionally, developing complementary LDH dynamic models will be critical in context of the emergence of *hrp2/hrp3* deletion, and a growing reliance on RDTs targeting pLDH [44, 45].

The persistence of *PfHRP2* and therefore the role of *PfHRP2*-based RDTs, including usRDTs, in low transmission and pre-elimination settings continues to be defined. This HRP2 model was developed using data from patients with low level parasitaemia and, therefore, provides a framework for further work simulating the levels of parasite density that maintain a detectable level of *PfHRP2*, depending on the LOD of the RDT and *PfHRP2* elimination half-life. How these relate to probability of transmission will help better inform the best use of usRDTs for the purpose of malaria elimination.

Another application of the model may be estimating the parasite biomass associated with severe malaria. Dondorp et al. showed that adults with severe malaria had a tenfold higher sequestered biomass, as calculated based on *PfHRP2* level, compared to adults with uncomplicated malaria [23]. In this study, patient specific weight and sex-based calculation of ECF improved the accuracy of the model compared with circulating blood volume alone, which might reflect this sequestration. However, further characterization of the dynamics of biomarker production by sequestered parasites is required to fully elucidate this link.

Conclusions

This study presenting an updated model of the dynamics of *PfHRP2* found that 33.6×10^{-15} g of *PfHRP2* was produced in vivo per parasite per life cycle and demonstrated a *PfHRP2* clearance half-life of 1.67 days in malaria naïve subjects infected with 3D7 *P. falciparum* parasites and treated with non-ACT anti-malarial agents. The performance of the model in predicting clearance of *PfHRP2* and likely duration of RDT positivity post artemisinin-based combination treatment of symptomatic malaria demonstrates the importance of understanding the dynamics of diagnostic biomarkers in order to inform optimal use of RDTs.

Abbreviations

ACT: Artemisinin-based combination therapy; BV: Blood volume; CI: Confidence interval; CRP: C-reactive protein; d_k : Proportion of *PfHRP2* remaining k days after it was produced; ECF: Extracellular fluid; ELISA: Enzyme linked immuno-sorbent assay; f : Amount of *PfHRP2* produced per parasite per lifecycle; H_t : Predicted absolute amount of *PfHRP2* circulating in the body at any day during an infection; IBSM: Induced blood stage malaria; IQR: Interquartile range; iRBC: Infected red blood cell; LDH: Lactate dehydrogenase; LOD: Limit of detection; m : Scaling factor; *PfHRP2*: *Plasmodium falciparum* histidine rich protein 2; p_j : Number of replicating parasites circulating in the host on the j th day; pLDH: Pan-*Plasmodium* lactate dehydrogenase; qPCR: Quantitative polymerase chain reaction; RDTs: Rapid diagnostic tests; RMSE: Root mean square error; rRNA: Ribosomal ribonucleic acid; RSS: Residual sum of squares; usRDT: Ultra-sensitive rapid diagnostic tests; $t_{1/2}$: Elimination half-life of *PfHRP2*; T_{max} : Predicted maximum concentration of circulating *PfHRP2*; T_{min} : Predicted minimum concentration of circulating *PfHRP2*; TRSS: Total residual sum of squares.

Supplementary Information

The online version contains supplementary material available at <https://doi.org/10.1186/s12936-022-04245-z>.

Additional file 1: Material S1. Anti-malarial treatment details for IBSM individuals. **Table S1.** Antimalarial treatment given for the 15 IBSM individuals from four different studies, as identified with the clinical trial name and clinical trial ID. The antimalarial and dose given at day of treatment on Day 7 is detailed for each subject. **Material S2.** Methods to fit *PfHRP2* model to the 6 individuals from the Namibia longitudinal cohort study. **Table S2.** Model performance of the Base model and red the Final model for the 15 IBSM individuals. Performance measures were the number (%) of *PfHRP2* observations within the range of the predicted minimum and maximum *PfHRP2* concentrations, the residual sum of squares (RSS) and the residual mean sum of square (RMSE). **Table S3.** Model performance of the updated model with *PfHRP2* half-life estimate of 1.67 days applied to 6 individuals aged between 23 and 27 years from the study in Namibia in participants with *Plasmodium falciparum* mono-infection. Performance measures were the number (%) of *PfHRP2* observations within the range of the predicted minimum and maximum *PfHRP2* concentrations, the residual sum of squares (RSS), residual mean sum of square (RMSE), the predicted and observed days above 800 or 80 pg/mL. **Figure S1.** Fits of the Base Model and the Final Model for the 15 IBSM individuals. The observed parasitemia over the course of infection is represented by black solid line, observed *PfHRP2* concentration is represented by circles (pre-treatment in solid circles and post-treatment in open circles), and the predicted minimum and maximum *PfHRP2* concentration from the model is shown as blue and red dashed lines, respectively. **Figure S2.** Simulated parasitemia growth and clearance over the course of the infection for each of the 6 individuals from the Namibia longitudinal cohort study is represented by the black line. The observed parasitemia (parasites/mL)

during the study are represented by the blue triangles and the replicating parasites used as input into the *PfHRP2* model are represented by open circles. **Figure S3.** Fits of the final model with elimination half-life of 1.67 days to the 6 individuals from the Namibia longitudinal cohort study, with observed *PfHRP2* concentration represented by closed circles, and minimum and maximum predicted *PfHRP2* concentration represented by the blue and red dashed lines, respectively. The dashed grey horizontal line represents the threshold of 800 pg/mL and the solid grey horizontal line represents the threshold of 80 pg/mL which correspond to the positivity threshold of an RDT and usRDT respectively.

Additional file 2. Includes the R codes and required datasets to perform the final HRP2 models as presented in the manuscript. Further details about the contents of R code and datasets are included in "File Details.txt".

Acknowledgements

We thank all the volunteers who participated in the studies and the staff at PATH for Quansys ELISA for biomarkers. For the IBSM studies we thank the staff at QIMR Berghofer Medical Research Institute who managed and prepared the *Plasmodium falciparum* 3D7 inoculum; clinical study team at Q-Pharm who conducted the trial; staff at the Queensland Paediatric Infectious Diseases laboratory for qPCR analysis; and Jörg Möhrle from MMV for permitting use of the data. For the Namibia longitudinal cohort study, the authors would like to thank the study participants, all field staff and field supervisors for the support with field implementation, all study staff, the local and national Namibia Ministry of Health and Social Services, and the University of Namibia for their support.

Author contributions

GJD and JSM conceptualized the study. LM and LW conducted analyses, updated the mathematical model and interpreted the data and model outputs. GJD, JSM, MLG, MK, POR and SB reviewed and interpreted model output. LM and SB drafted the manuscript, with substantial input in drafting phases from POR, LW, JSM and GJD. IKJ performed the laboratory testing of RDTs and Quansys assays, and interpretation of data. MSH, HN and DRM provided data from Namibia study and interpretation of data. All authors contributed to the writing and review of the manuscript. All authors read and approved the final manuscript.

Funding

This work was supported, in whole or in part, by the Bill & Melinda Gates Foundation (Grant Numbers: 347 OPP1135840 and A128488). Under the grant conditions of the Foundation, a Creative Commons Attribution 4.0 Generic License has already been assigned to the Author Accepted Manuscript version that might arise from this submission.

This work for the IBSM studies was financially supported by Medicines for Malaria Venture through a Wellcome Trust grant (reference number 095909/Z/11/Z), a grant by the Global Health Innovation and Technology Fund (GHIT) (Grant No. G2014-108), and by funding from the Bill and Melinda Gates Foundation. Antigen quantification work conducted at PATH was supported by an award to PATH in whole by the Bill & Melinda Gates Foundation [Grant Number 347 OPP1135840]. The Namibia Cohort Study was funded by the Bill and Melinda Gates Foundation (A128488) and University of Texas Southwestern Department of Pediatrics Horchow Family Fund (5300375400). JSM was supported by an Australian government National Health and Medical Research Council (NHMRC) Practitioner Fellowship (APP1135955) and supported by an NHMRC Program Grant (1132975).

Availability of data and materials

The datasets used and analysed during the current study are included in this published article and its Additional files. The R code of the final *PfHRP2* model for the IBSM study and the Namibia Cohort Study are included as Additional file 2.

Declarations

Ethics approval and consent to participate

The IBSM studies were approved by the QIMR Berghofer Medical Research Institute Human Research Ethics Committee. The study protocol for the

Namibia longitudinal cohort study was approved by the Research Unit of the Ministry of Health and Social Services of Namibia, the University of Namibia Research Ethics Committee and the University of California, San Francisco Committee for Human Research. All participants recruited for the study or their parents/guardians provided written consent.

Consent for publication

Not applicable.

Competing interests

All authors declare that they have no competing interests.

Author details

¹QIMR Berghofer Medical Research Institute, Brisbane, QLD, Australia. ²University of Queensland, Brisbane, QLD, Australia. ³Queensland University of Technology, Brisbane, QLD, Australia. ⁴Department of Pediatrics, University of Texas, Southwestern, Dallas, TX, USA. ⁵Malaria Elimination Initiative, Institute for Global Health Services, University of California, San Francisco, CA, USA. ⁶Department of Pediatrics, University of California, San Francisco, CA, USA. ⁷Diagnostics Program, PATH, Seattle, WA, USA. ⁸Multidisciplinary Research Centre, University of Namibia, Windhoek, Namibia.

Received: 12 August 2021 Accepted: 13 July 2022

Published online: 03 August 2022

References

- Jimenez A, Rees-Channer RR, Perera R, Gamboa D, Chiodini PL, Gonzalez IJ, et al. Analytical sensitivity of current best-in-class malaria rapid diagnostic tests. *Malar J*. 2017;16:128.
- Roberts L, Enserink M. Malaria. Did they really say ... eradication? *Science*. 2007;318:1544–5.
- Slater HC, Ross A, Ouedraogo AL, White LJ, Nguon C, Walker PG, et al. Assessing the impact of next-generation rapid diagnostic tests on *Plasmodium falciparum* malaria elimination strategies. *Nature*. 2015;528:S94–101.
- Cook J, Xu W, Msellem M, Vonk M, Bergstrom B, Gosling R, et al. Mass screening and treatment on the basis of results of a *Plasmodium falciparum*-specific rapid diagnostic test did not reduce malaria incidence in Zanzibar. *J Infect Dis*. 2015;211:1476–83.
- Hsiang MS, Ntshalintshali N, Kang Dufour MS, Dlamini N, Nhlabathi N, Vilakati S, et al. Active case finding for malaria: a 3-year national evaluation of optimal approaches to detect infections and hotspots through reactive case detection in the low-transmission setting of Eswatini. *Clin Infect Dis*. 2020;70:1316–25.
- WHO. Guidelines for the treatment of malaria. Geneva: World Health Organization; 2010.
- Tjitra E, Suprianto S, McBroom J, Currie BJ, Anstey NM. Persistent ICT malaria Pf/Pv panmalarial and HRP2 antigen reactivity after treatment of *Plasmodium falciparum* malaria is associated with gametocytemia and results in false-positive diagnoses of *Plasmodium vivax* in convalescence. *J Clin Microbiol*. 2001;39:1025–31.
- Dalrymple U, Arambepola R, Gething PW, Cameron E. How long do rapid diagnostic tests remain positive after anti-malarial treatment? *Malar J*. 2018;17:228.
- Mtove G, Nadjm B, Amos B, Hendriksen IC, Muro F, Reyburn H. Use of an HRP2-based rapid diagnostic test to guide treatment of children admitted to hospital in a malaria-endemic area of north-east Tanzania. *Trop Med Int Health*. 2011;16:545–50.
- Kyabayinze DJ, Tibenderana JK, Odong GW, Rwakimari JB, Counihan H. Operational accuracy and comparative persistent antigenicity of HRP2 rapid diagnostic tests for *Plasmodium falciparum* malaria in a hyperendemic region of Uganda. *Malar J*. 2008;7:221.
- Kattenberg JH, Tahita CM, Versteeg IA, Tinto H, Traore-Coulibaly M, Schallig HD, Mens PF. Antigen persistence of rapid diagnostic tests in pregnant women in Nanoro, Burkina Faso, and the implications for the diagnosis of malaria in pregnancy. *Trop Med Int Health*. 2012;17:550–7.
- Nkonya DN, Tarimo DS, Kishimba RS. Accuracy of clinical diagnosis and malaria rapid diagnostic test and its influence on the management of

- children with fever under reduced malaria burden in Misungwi district, Mwanza Tanzania. *Pan Afr Med J*. 2016;25:48.
13. Joshi R, Colford JM Jr, Reingold AL, Kalantri S. Nonmalarial acute undifferentiated fever in a rural hospital in central India: diagnostic uncertainty and overtreatment with antimalarial agents. *Am J Trop Med Hyg*. 2008;78:393–9.
 14. Dalrymple U, Cameron E, Arambepola R, Battle KE, Chestnutt EG, Keddie SH, et al. The contribution of non-malarial febrile illness co-infections to *Plasmodium falciparum* case counts in health facilities in sub-Saharan Africa. *Malar J*. 2019;18:195.
 15. Das S, Jang IK, Barney B, Peck R, Rek JC, Arinaitwe E, et al. Performance of a high-sensitivity rapid diagnostic test for *Plasmodium falciparum* malaria in asymptomatic individuals from Uganda and Myanmar and naive human challenge infections. *Am J Trop Med Hyg*. 2017;97:1540–50.
 16. Akinyi S, Hayden T, Gamboa D, Torres K, Bendezu J, Abdallah JF, et al. Multiple genetic origins of histidine-rich protein 2 gene deletion in *Plasmodium falciparum* parasites from Peru. *Sci Rep*. 2013;3:2797.
 17. Koita OA, Doumbo OK, Ouattara A, Tall LK, Konare A, Diakite M, et al. False-negative rapid diagnostic tests for malaria and deletion of the histidine-rich repeat region of the hrp2 gene. *Am J Trop Med Hyg*. 2012;86:194–8.
 18. Howard RJ, Uni S, Aikawa M, Aley SB, Leech JH, Lew AM, et al. Secretion of a malarial histidine-rich protein (Pf HRP II) from *Plasmodium falciparum*-infected erythrocytes. *J Cell Biol*. 1986;103:1269–77.
 19. Desakorn V, Dondorp AM, Silamut K, Pongtavornpinyo W, Sahassananda D, Chotivanich K, et al. Stage-dependent production and release of histidine-rich protein 2 by *Plasmodium falciparum*. *Trans R Soc Trop Med Hyg*. 2005;99:517–24.
 20. Poti KE, Balaban AE, Pal P, Kobayashi T, Goldberg DE, Sinnis P, et al. In vivo compartmental kinetics of *Plasmodium falciparum* histidine-rich protein II in the blood of humans and in BALB/c mice infected with a transgenic *Plasmodium berghei* parasite expressing histidine-rich protein II. *Malar J*. 2019;18:78.
 21. Barber BE, William T, Grigg MJ, Parameswaran U, Piera KA, Price RN, et al. Parasite biomass-related inflammation, endothelial activation, microvascular dysfunction and disease severity in vivax malaria. *PLoS Pathog*. 2015;11: e1004558.
 22. Hendriksen IC, Mwanga-Amumpaire J, von Seidlein L, Mtove G, White LJ, Olaosebikan R, et al. Diagnosing severe falciparum malaria in parasitaemic African children: a prospective evaluation of plasma PfHRP2 measurement. *PLoS Med*. 2012;9: e1001297.
 23. Dondorp AM, Desakorn V, Pongtavornpinyo W, Sahassananda D, Silamut K, Chotivanich K, et al. Estimation of the total parasite biomass in acute falciparum malaria from plasma PfHRP2. *PLoS Med*. 2005;2: e204.
 24. Plucinski MM, Dimbu PR, Fortes F, Abdulla S, Ahmed S, Gutman J, et al. Posttreatment HRP2 clearance in patients with uncomplicated *Plasmodium falciparum* malaria. *J Infect Dis*. 2018;217:685–92.
 25. Marquart L, Butterworth A, McCarthy JS, Gatton ML. Modelling the dynamics of *Plasmodium falciparum* histidine-rich protein 2 in human malaria to better understand malaria rapid diagnostic test performance. *Malar J*. 2012;11:74.
 26. Jang IK, Tyler A, Lyman C, Kahn M, Kalnoky M, Rek JC, et al. Simultaneous quantification of *Plasmodium* antigens and host factor C-reactive protein in asymptomatic individuals with confirmed malaria by use of a novel multiplex immunoassay. *J Clin Microbiol*. 2019;57:e00948-18.
 27. McCarthy JS, Ruckle T, Elliott SL, Ballard E, Collins KA, Marquart L, et al. A single-dose combination study with the experimental antimalarials artefenomel and DSM265 to determine safety and antimalarial activity against blood-stage *Plasmodium falciparum* in healthy volunteers. *Antimicrob Agents Chemother*. 2019;64:e01371-19.
 28. Collins KA, Wang CY, Adams M, Mitchell H, Rampton M, Elliott S, et al. A controlled human malaria infection model enabling evaluation of transmission-blocking interventions. *J Clin Invest*. 2018;128:1551–62.
 29. Collins KA, Ruckle T, Elliott S, Marquart L, Ballard E, Chalou S, et al. DSM265 at 400 milligrams clears asexual stage parasites but not mature gametocytes from the blood of healthy subjects experimentally infected with *Plasmodium falciparum*. *Antimicrob Agents Chemother*. 2019;63:e01371-19.
 30. Isozumi R, Fukui M, Kaneko A, Chan CW, Kawamoto F, Kimura M. Improved detection of malaria cases in island settings of Vanuatu and Kenya by PCR that targets the *Plasmodium* mitochondrial cytochrome c oxidase III (cox3) gene. *Parasitol Int*. 2015;64:304–8.
 31. Araar A, Levine S, Duclos J-Y. Body mass index, poverty and inequality in Namibia. Paper prepared for Central Bureau of Statistics. Namibia; 2009.
 32. Ho MF, Baker J, Lee N, Luchavez J, Arie F, Nhem S, et al. Circulating antibodies against *Plasmodium falciparum* histidine-rich proteins 2 interfere with antigen detection by rapid diagnostic tests. *Malar J*. 2014;13:480.
 33. Wang CYT, Ballard EL, Pava Z, Marquart L, Gaydon J, Murphy SC, et al. Analytical validation of a real-time hydrolysis probe PCR assay for quantifying *Plasmodium falciparum* parasites in experimentally infected human adults. *Malar J*. 2021;20:181.
 34. Hofmann N, Mwingira F, Shekalaghe S, Robinson LJ, Mueller I, Felger I. Ultra-sensitive detection of *Plasmodium falciparum* by amplification of multi-copy subtelomeric targets. *PLoS Med*. 2015;12: e1001788.
 35. Wockner LF, Hoffmann I, Webb L, Mordmuller B, Murphy SC, Kublin JG, et al. Growth rate of *Plasmodium falciparum*: analysis of parasite growth data from malaria volunteer infection studies. *J Infect Dis*. 2020;221:963–72.
 36. Boer P. Estimated lean body mass as an index for normalization of body fluid volumes in humans. *Am J Physiol*. 1984;247:F632–6.
 37. Guyton AC, Hall JE. Textbook of medical physiology. 11th ed. Pennsylvania: Elsevier Saunders; 2006.
 38. Stepniewska K, Ashley E, Lee SJ, Anstey N, Barnes KI, Binh TQ, et al. In vivo parasitological measures of artemisinin susceptibility. *J Infect Dis*. 2010;201:570–9.
 39. Dahal P, d'Alessandro U, Dorsey G, Guerin PJ, Nsanabana C, WWARN Artemisinin-based Combination Therapy Africa Baseline Group, et al. Clinical determinants of early parasitological response to ACTs in African patients with uncomplicated falciparum malaria: a literature review and meta-analysis of individual patient data. *BMC Med*. 2015;13:212.
 40. Singh N, Shukla MM. Short report: Field evaluation of posttreatment sensitivity for monitoring parasite clearance of *Plasmodium falciparum* malaria by use of the determine malaria pf test in central India. *Am J Trop Med Hyg*. 2002;66:314–6.
 41. Aydin-Schmidt B, Mubi M, Morris U, Petzold M, Ngasala BE, Premji Z, et al. Usefulness of *Plasmodium falciparum*-specific rapid diagnostic tests for assessment of parasite clearance and detection of recurrent infections after artemisinin-based combination therapy. *Malar J*. 2013;12:349.
 42. Hayward RE, Sullivan DJ, Day KP. *Plasmodium falciparum*: histidine-rich protein II is expressed during gametocyte development. *Exp Parasitol*. 2000;96:139–46.
 43. Reichert EN, Hume JCC, Sagara I, Healy SA, Assadou MH, Guindo MA, et al. Ultra-sensitive RDT performance and antigen dynamics in a high-transmission *Plasmodium falciparum* setting in Mali. *Malar J*. 2020;19:323.
 44. Gatton ML, Chaudhry A, Glenn J, Wilson S, Ah Y, Kong A, et al. Impact of *Plasmodium falciparum* gene deletions on malaria rapid diagnostic test performance. *Malar J*. 2020;19:392.
 45. Thomson R, Parr JB, Cheng Q, Chenet S, Perkins M, Cunningham J. Prevalence of *Plasmodium falciparum* lacking histidine-rich proteins 2 and 3: a systematic review. *Bull World Health Organ*. 2020;98:558–68.

Publisher's Note

Springer Nature remains neutral with regard to jurisdictional claims in published maps and institutional affiliations.

Ready to submit your research? Choose BMC and benefit from:

- fast, convenient online submission
- thorough peer review by experienced researchers in your field
- rapid publication on acceptance
- support for research data, including large and complex data types
- gold Open Access which fosters wider collaboration and increased citations
- maximum visibility for your research: over 100M website views per year

At BMC, research is always in progress.

Learn more biomedcentral.com/submissions

